

# Dynamic Properties of Short Fiber–EPDM Matrix Composites as a Function of Strain Amplitude

L. IBARRA

Instituto de Ciencia y Tecnología de Polímeros C.S.I.C., c/ Juan de la Cierva 3, 28006 Madrid, Spain

## SYNOPSIS

The dynamic properties of composite materials consisting of an ethylene–propylene rubber matrix (EPDM) and short polyester polyethylene-terephthalate (PET) fiber vary with dynamic stress amplitude applied to the material. These variations support the statement that fiber treatment with 1,4-carboxy-sulphonyl-diazide, which acts as a bridge between the fiber and the matrix and hence enhances the strength of the interface enabling it to resist greater strain applied to the composite and, as a consequence, yielding greater retention values of the storage modulus, measured longitudinally to preferential fiber orientation,  $E'_L$ . By means of transversal measurements of the storage modulus,  $E'_T$ , of these materials it is possible to determine a parameter  $b$ , which eventually indicates the degree of matrix–fiber bonding and which is consistently higher for materials filled with surface-treated fiber. This enhanced phase adhesion is further confirmed by higher equivalent interfacial thickness values,  $\Delta R$ , which, in addition, vary less with increasing dynamic strain amplitude. Finally dissipated energy variation or mechanical energy loss,  $E_{\text{loss}}$ , is studied as a function of fiber content and strain amplitude. Experimental findings show  $E_{\text{loss}}$  to increase with fiber content and strain amplitude, when measured at constant strain amplitude  $\epsilon_0$ , and to yield higher values for treated fiber samples. © 1994 John Wiley & Sons, Inc.

## INTRODUCTION

Elastomer reinforcement with short fiber is of great practical and economic interest for the rubber industry, as it provides, in principle, for a simple way of manufacturing reinforced rubber commodities. The benefit of these composite materials consisting of short fiber and an elastomeric matrix is that they combine the flexibility of the matrix with the strength and rigidity of the reinforcing fiber, apart from the anisotropic characteristics of the resulting material properties.

In general the enhanced properties of these composites are attributed to the strength of the interface, which is due to the presence of different types of bonding agents, among which the three-component dry system (silica, phenol, formaldehyde)<sup>1</sup> deserves special mention, as well as the system RFL,<sup>2</sup> both

of which generate matrix–fiber crosslinks. These are mainly physical links of varying strength, the ideal case arising where the two phases adhere by means of truly chemical and covalent bonds.

One of the most important aspects in the manufacture of these materials is to achieve good fiber–matrix adhesion. Most of the attempts to solve this problem refer to grafting reactions on the fiber surface,<sup>3,4</sup> the incorporation of coupling agents into the elastomeric blend,<sup>5</sup> or fiber pretreatment with these agents.<sup>6</sup> Yet correct assessment of the existence of phase adhesion still remains a problem.

In the literature dealing with short fiber-reinforced materials, recourse is taken to scanning electron microscopy (SEM) when testing for phase adhesion<sup>7,8</sup> or else to measurements of solvent swelling loss<sup>9,10</sup> or dynamic property measurements,<sup>11,12</sup> and, in recent times, to measuring the stresses occurring during fiber pull-out.<sup>13,14</sup> On the whole, however, there exist relatively few publications on this particular aspect.

In recent research the authors endeavored to generate chemical bonds between the fiber and the matrix by taking advantage of the reactivity of the azide group  $—N_3$ , thus functionalizing short polyester polyethylene-terephthalate (PET),<sup>15,16</sup> polyamide,<sup>17</sup> and carbon<sup>18</sup> fibers. With the aim of further pursuing the course undertaken, in this research the dynamic properties are examined as a function of strain amplitude in composite materials consisting of an ethylene-propylene rubber matrix (EPDM) and short polyester PET fiber, pretreated with *p*-sulphonyl-carbonyl-diazone in such a way that the fibers possess a sulphonylazide group,  $—SO_2N_3$ , capable of reacting with the elastomeric matrix during the curing process and creating a true covalent bond between both.

In this work, the effect of fiber content in the material is determined and comparison is made with other similar composites containing untreated fiber.

## EXPERIMENTAL

### Materials

The basic elastomer was a Montedison EPDM Dutral TER 054E, with the following significant characteristics: Oil content 0%, approximate propylene content 50%, Mooney viscosity in the order of 40 units. The third monomer has a normal, mildly unsaturated ethylidene-norbornene level; specific weight 0.865.

The fiber used was polyester PET supplied by Velutex Floc S.A. Company, mean length 6 mm, specific weight 1.38, and mean diameter 18  $\mu$ m. For surface treatment 1,4-carboxy-sulphonyl-diazone was used, which was prepared according to the method developed in our laboratory, as described elsewhere<sup>15</sup> and using commercial raw materials.

### Blend Preparation and Curing

Blends were prepared incorporating treated and untreated fiber, in the amounts indicated below:

Dutral TER 054E	100
Zinc oxide	5
Stearic acid	3
Black N-660	40
TMTD accelerant	0.5
MBT accelerant	0.5
ZDBC accelerant	1
Sulfur	1
Variable portions of polyester PET fiber	

the different materials being identified according to the following breakdown:

Fiber Volume	Untreated Fiber	Treated Fiber
2	C-2	C-6
5	C-3	C-7
8	C-4	C-8
10	C-5	C-9

plus a fiber-free blend referred to as control or C-1.

The blends were prepared in a 12-in. laboratory roller mixer with a friction ratio of 1 : 1.25 and at a temperature of 70°C.

First the fiber-free blend was prepared following conventional practice. Subsequently the fiber was added taking care that the flow direction of the blend always adjusted to roller rotation, even when it had to be remixed with itself, to the purpose of favoring fiber orientation to a maximum following roller direction, even in the deeper matrix layers.

Once the blends had been prepared, they were cured in a press heated by thermofluid at a temperature of 160°C and at the curing times determined as optimal by the rheometer.

### Measurement of Dynamic Properties

Dynamic property measurements were conducted in a Metravib Viscoanalyzer RAC 815A at variable dynamic strain at a temperature of 23°C and a frequency of 10 Hz, utilizing parallelepipedic samples dimensioned 16 × 16 × 4 mm.

These properties were measured in two directions as determined by preferential fiber orientation: longitudinal (*L*) and transversal (*T*). Sample preparation with fibers oriented preferentially in these two directions did not pose any problem at all: It was sufficient to follow the flow direction of the blend.

## RESULTS AND DISCUSSION

### Dynamic Properties

Figure 1 shows storage modulus  $E'$  variation as a function of fiber content in the composite, longitudinally (fat line) and perpendicularly (dotted line) to preferential fiber orientation, for treated and untreated fiber.

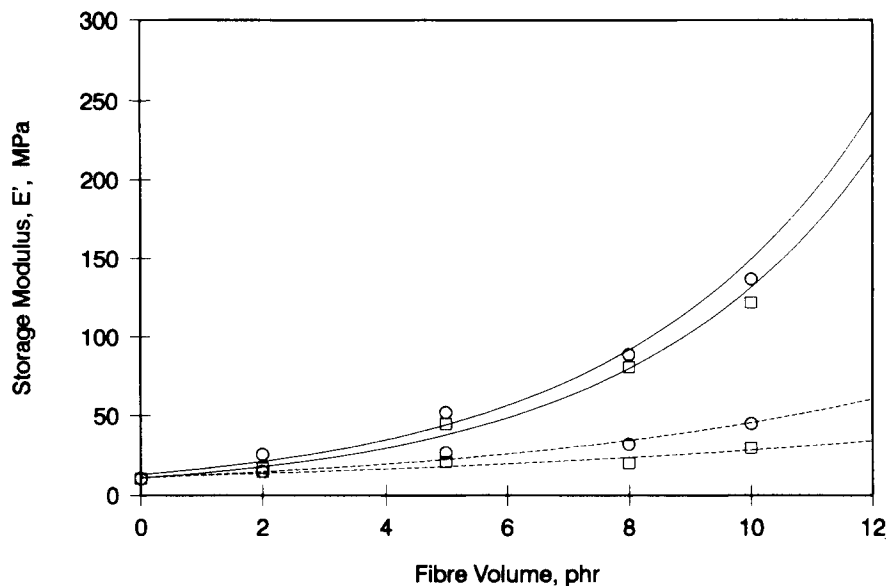


**Figure 1** Modulus  $E'$  variation in the linear response zone as a function of fiber content: (—) longitudinal measurements; (---) transversal measurements. (○) Materials containing treated fiber; (□) materials filled with untreated fiber. Vibration frequency: 10 Hz.

For both composite types the same behavior is observed. In fact, independent of fiber direction,  $E'$  increases with fiber content, although the increase is more significant when strain is applied longitudinally,  $L$ , than when applied perpendicularly,  $T$ , which evidences the anisotropy of this property in the experimental composites.

In addition, the  $E'$  values are observed to be consistently higher in the treated fiber composites, independent of fiber content and measurement direction. It is noteworthy, however, that for longitudinal measurements the  $E'$  differential existing for one and the same fiber content between treated and untreated fiber samples remains practically constant, whereas in transversal measurements, the modulus differential increases with increasing fiber portion in the material.

Figure 2 shows storage modulus variation, in longitudinal measurements,  $E'_L$ , plotted against strain amplitude, in terms of double strain amplitude (DSA). All samples show identical behavior: There is a linear response area of the modulus, where it is independent of strain amplitude, until a strain threshold, as of which the modulus progressively diminishes. With increasing fiber content the linear response zone is being narrowed, a phenomenon which becomes more prominent for high fiber content samples.

The effect of strain increase on modulus  $E'$  has been widely studied in particle-filled samples,<sup>19</sup> for

which the observed decrease is attributed to the rupture of physical links between the filler and the matrix. In fiber-reinforced materials modulus decrease has also been observed,<sup>20</sup> which by the same token may also be attributed to the total ruptures of physical interactions between the reinforcing material, filler and fiber, and the matrix.

Table I compiles the storage modulus values in longitudinal measurements, corresponding to the highest strain amplitudes achieved in the assays,  $E'_{L,F}$ , for the different composites, grouped according to fiber content. As can be observed, for any fiber portion, modulus  $E'$  is consistently higher in the treated-fiber composites. In addition, the modulus differential between the linear response zone  $E'_{L,0}$  and the drop,  $E'_{L,F}$  has been taken into account, the right hand column of Table I listing the modulus drop/strain ratios, which are always smaller for the treated fiber materials and increase proportionate to fiber content, and in all cases are higher than the value recorded for the matrix.

The values of the loss factor  $\tan \delta$  are recorded in Table II, as longitudinal measurements for each of the experimental materials and at two different strain amplitudes: That of the linear response zone,  $\tan \delta_0$  and the final amplitude reached experimentally,  $\tan \delta_f$ .

In all cases the composite materials present a lower damping capacity than the fiber-free matrix, which still decreases with increasing fiber portion.

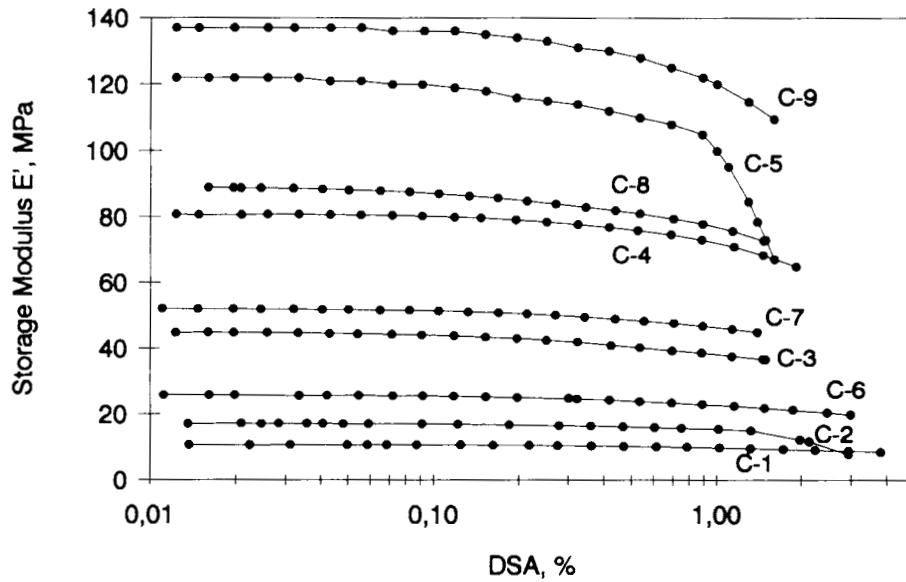


**Figure 2** Storage modulus variation with strain amplitude. Measurements taken longitudinally to preferential fiber orientation in the matrix.

In the treated fiber samples the loss factor is lower than in the respective untreated fiber composites, at any strain amplitude.

The effect of increases in strain amplitude on the loss factor has been studied for polymers filled with coupling agents of the silane type<sup>21</sup> reporting a marked influence of surface treatment. For fiber-reinforced materials in all cases  $\tan \delta$  is observed to increase proportionate to strain increase. The last column in Table II shows the  $\tan \delta$  increases obtained as the differential between  $\tan \delta_F$  and  $\tan \delta_0$ . It can be observed that the loss factor increase is consistently lower in the samples filled with surface-treated fiber. This means that, when strain is applied longitudinally to the preferential fiber orientation, the interface is strong enough to resist substantial deformation, owing to the fiber-matrix bonds gen-

erated through fiber surface modification. In other words, for one and the same stress material rupture is lower for materials filled with surface-treated fiber.

Figure 3 shows storage modulus variation  $E'_T$  measured perpendicularly to fiber orientation, as a function of strain amplitude and for all the experimental materials. On the whole the behavior is similar to that in longitudinal measurements, although the linear response zone appears to be expanded, especially for high fiber content. In addition, for one and the same fiber portion, material differences are more prominent.

**Matrix-Fiber Interface**

Figure 4 shows the values of the elastic modulus  $E'_T$ , measured transversally, as a function of fiber

**Table I**  $E'_L$  Variation with Strain Amplitude

Sample	DSA <sub>F</sub> , %	$E'_{L,F}$ , MPa	$E'_{L,0}-E'_{L,F}$	Slope
C-1	3	8.79	1.79	0.59
C-2	3	7.66	9.34	3.11
C-6	3	19.8	5.9	1.97
C-3	1.5	36.6	8.2	5.5
C-7	1.5	44.8	7.2	4.8
C-4	1.5	68.5	12.3	8.2
C-8	1.5	72.65	16.35	10.9
C-5	1	100	22	22
C-9	1	120.3	16.7	16.7

**Table II**  $\tan \delta$  Variation with Strain Amplitude

Sample	DSA <sub>F</sub> , %	$\tan \delta_0$	$\tan \delta_F$	$\Delta \tan \delta$
C-1	3	0.066	0.096	0.03
C-2	3	0.053	0.106	0.053
C-6	3	0.065	0.096	0.031
C-3	1.5	0.056	0.084	0.028
C-7	1.5	0.044	0.066	0.022
C-4	1.5	0.046	0.070	0.024
C-8	1.5	0.041	0.064	0.023
C-5	1	0.041	0.066	0.025
C-9	1	0.039	0.057	0.018

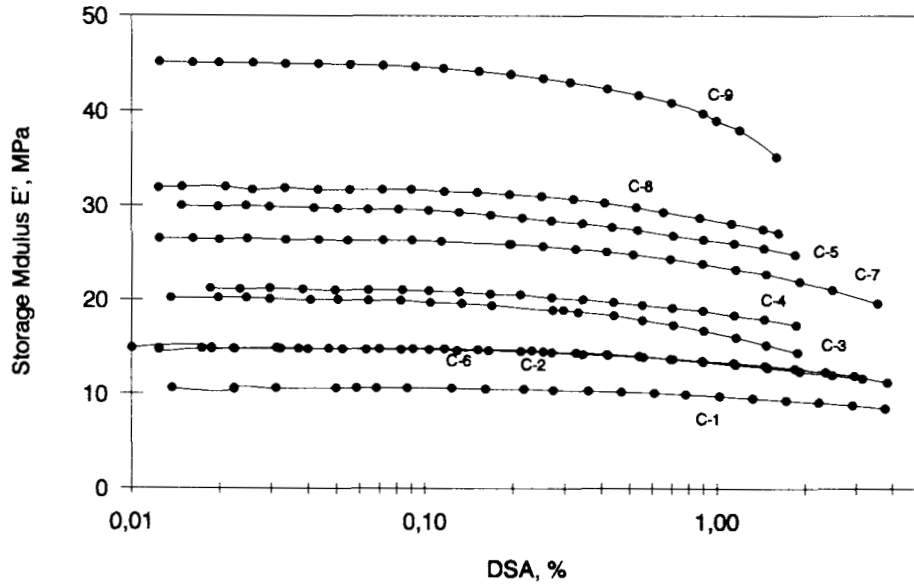


**Figure 3** Storage modulus variation with strain amplitude. Transversal measurements in respect of preferential fiber orientation in the matrix.

volume in percent,  $V_f$ , for both treated and untreated fiber samples. The modulus value is observed to grow linearly with fiber content, a fact described in the following expression:<sup>22</sup>

$$\log E'_T = a + bV_f \quad (1)$$

where  $a$  and  $b$  are constants. It is well known that for many materials consisting of two phases, the

modulus can be expressed by means of the “logarithmic blend rule,” according to the following equation:

$$\begin{aligned} \log E'_c &= V_m \cdot \log E'_m + V_f \cdot \log E'_f \\ &= \log E'_m + V_f \cdot \log (E'_f/E'_m) \end{aligned} \quad (2)$$

where the subscripts  $c$ ,  $m$ , and  $f$  refer to the com-

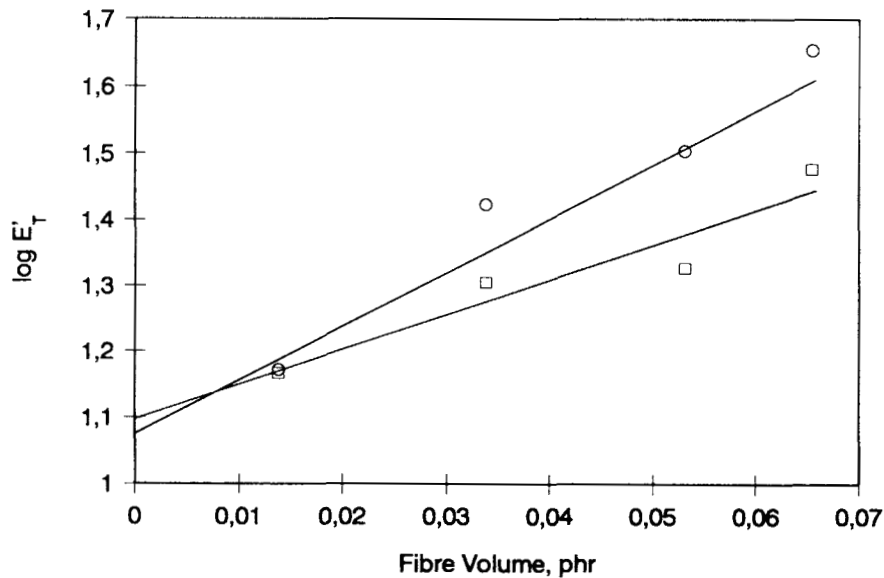


**Figure 4** Effect of the fiber portion on the transversal storing modulus  $E'_T$ : (O) treated fiber composites; (□) untreated fiber materials.

posite, matrix, and fiber, respectively. Comparing Eq. (1) and (2), the value of  $a$  corresponds to  $\log E'_m$  and that of  $b$  to  $\log E'_f/E'_m$ .

By means of least-square adjustment the values of the slope and the  $Y$  intercept are determined, as corresponding to  $b$  and  $a$ , respectively. The values of these parameters are indicated in the following:

	$a$	$b$
Untreated	1.097	5.30
Treated	1.075	8.75

On the one hand the value of  $a$  in both cases is in good agreement with the measured logarithm of  $E'_M$  (1.025), but there exists a notable difference for the  $b$  values.

When the ratio between  $b$  and  $\log E'_f/E'_m$  is represented as a function of  $\gamma$ ,  $b$  is expressed as follows:

$$b = \gamma \cdot \log(E'_f/E'_m)$$

where the value of  $\gamma$  is a factor indicating the degree of fiber-matrix bonding, i.e., the higher the value of  $\gamma$ , the stronger becomes phase adhesion. Hence, the highest  $b$  value observed for composites filled with treated fiber can only be interpreted in terms of the existence of a stronger matrix-fiber interface favored by matrix-fiber bonding through the  $\text{SO}_2\text{N}_3$  groups present on the surface of the treated fiber.

Zhou et al.,<sup>23</sup> introduce a new concept, *equivalent interfacial thickness*, for the purpose of quantifying interfacial adhesion. They assume that the changes in the properties of a short fiber-reinforced rubber, attributable to interfacial action, are due to an increase in fiber radius, defined as  $\Delta R$  or equivalent interfacial thickness. This concept takes up the idea that the interface may be considered a uniform layer. Hence a higher  $\Delta R$  value refers to stronger interfacial action.

The Halpin-Tsai equation:

$$\frac{E'_T}{E'_M} = \frac{1 + 2\eta_T V_f}{1 - \eta_T V_f} \quad (3)$$

where  $E'_T$  is the storage modulus of the composite measured transversally,  $E'_M$  that of the matrix.  $V_f$  stands for the fiber volume fraction and  $\eta_T$  is the parameter to be entailed via introduction of the concept of equivalent interfacial thickness, may be rewritten as:

$$\frac{E'_T}{E'_M} = \frac{1 + 2V'_f}{1 - V'_f} \quad (4)$$

where  $V'_f$  is the equivalent fiber volume fraction. If  $B$  is defined, in the light of the preceding equations, as

$$B = \frac{V'_f}{V_f} = 1 + \left(\frac{\Delta R}{R_0}\right)^2 \quad (5)$$

where  $R_0$  is the fiber radius, the following expression can be obtained:

$$\frac{(E'_T/E'_M) - 1}{(E'_T/E'_M) + 2} = B V_f \quad (6)$$

From this latter equation the value of  $B$  can be determined and hence  $\Delta R$ :

$$\Delta R = R_0(\sqrt{B-1}) \quad (7)$$

In this research the  $\Delta R$  values were calculated for all the experimental samples, with the  $E'_T$  values corresponding to the linear response zone of the modulus, as compiled in Table III. These values demonstrate that for any fiber portion higher  $\Delta R$  values are obtained, which points toward greater interfacial action for treated fibers. In addition, these values are homogeneous and hence independent of fiber volume.

If  $\Delta R$  is determined for each sample as a function of dynamic strain (% DSA), the intersects obtained adjust to a negative slope straight line (cf. Fig. 5), i.e., the  $\Delta R$  value diminishes with increasing strain. The slopes obtained are compiled in Table IV.

In any case, for the treated fiber samples, the slopes obtained are always less steep, apart from showing a progressive flattening as a consequence of higher fiber content. This latter fact supports the assumption that the interface with treated fibers remains stable with increasing strain and hence the modulus is maintained also, which confirms our

**Table III**  $\Delta R$  Values as a Function of Fiber Volume

Fiber Volume	Untreated	Treated
2	24.9	25.3
5	22.8	26.9
8	16.7	23.2
10	19.8	23.8

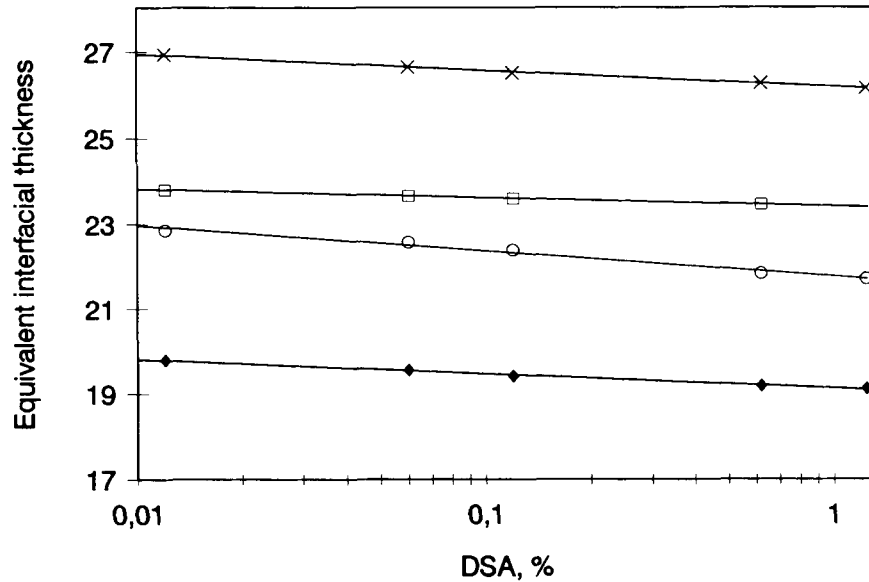


Figure 5 Equivalent interfacial thickness variation,  $\Delta R$ , as a function of dynamic strain amplitude. (○) C-3; (◆) C-5; (X) C-7; (□) C-9.

previous finding of lesser storage modulus drop at increasing strain amplitude.

**Energy Dissipation**

When a material is subjected to cyclic strain, part of the energy supplied is dissipated in the material and converted into heat, the remainder being returned to the system. This energy dissipation or, in other words, loss of mechanical energy is preferably applied in damping systems that absorb vibrations of either mechanical or acoustic nature.

Theoretically, the energy loss,  $E_{loss}$ , of a material subjected to cyclic strain is described in the following expression.<sup>24</sup>

$$E_{loss} = \pi |\sigma_0| \epsilon_0 |\sin \delta|$$

where  $\sigma_0$  is the stress amplitude,  $\epsilon_0$  being the strain amplitude. Taking into account that  $\sigma_0 = E^* \epsilon_0$  and

that  $\sin \delta = E''/E^*$ , the above expression can be rewritten as

$$E_{loss} = \pi |\sigma_0^2| D'' = \pi \epsilon_0^2 |E''$$

where  $D''$  stands for loss compliance ( $D'' = E''/E^{*2}$ ).

This latter expression allows for the inference that, at equal strain,  $E_{loss}$  will be proportionate to the loss modulus  $E''$ , and that for one and the same stress deformation,  $E_{loss}$  will be proportionate to the loss compliance,  $D''$ . Hence, if two materials are to be differentiated as to their dissipated energy, the type of deformation implied has to be taken into account.

Figures 6 and 7 show the energy loss variations as a function of fiber content in the composite, for constant strain and stress amplitudes, respectively.

These figures prove energy loss to increase with fiber content, as well as the anisotropy of the composite at constant fiber content. By the same token it is demonstrated that when defining energy loss, the type of deformation has to be differentiated in terms of constant stress or strain, as the figures prove that material hierarchy is inverted depending on the source of energy dissipation.

For one and the same strain amplitude, the results obtained confirm the data reported in the literature<sup>25</sup> regarding styrene-butadiene rubber (SBR) matrices, in the sense that when there exist bonds between the matrix and the fiber a shearing effect is generated

**Table IV Slopes of the Straight Lines Obtained by Plotting  $\Delta R$  Variations vs. Strain Amplitude**

Fiber Volume	Untreated	Treated
2	0.44	0.39
5	0.26	0.16
8	0.30	0.12
10	0.15	0.08

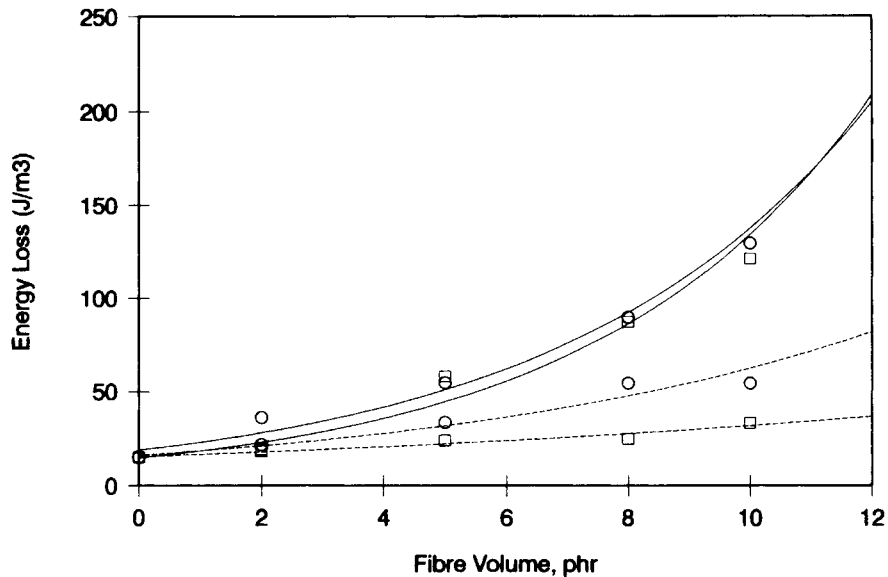


**Figure 6** Mechanical energy loss variation as a function of fiber content.  $\epsilon_0 = 0.005$ , vibration frequency 10 Hz. Symbols as in Figure 1.

at the interface that enhances the mechanical energy loss variation at constant strain. In addition, energy loss variation is shown to correlate to storage modulus variation. Hence the similarity between the graphs in Figure 1 and 6.

In Figures 8 and 9 the energy loss variation has been plotted against strain and stress amplitude, respectively, for the composites containing different

amounts of treated fiber. As can be observed, energy loss, or else energy dissipation, increases linearly with either stress or strain amplitude. When increasing the fiber portion, the results differ according to the deformation type. In fact, for variable-strain amplitude, the dissipated energy value increases proportionate to fiber content. The inverse occurs when measuring at variable stress amplitude.

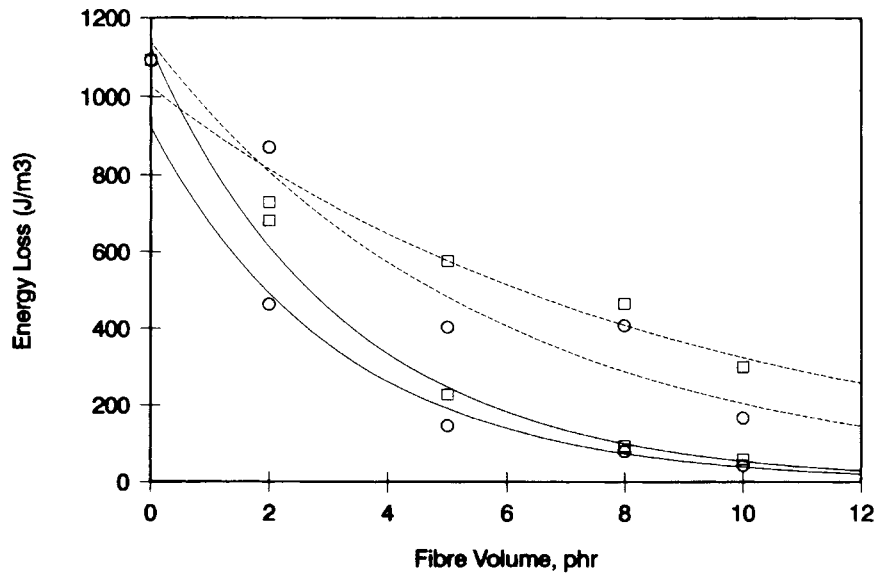


**Figure 7** Mechanical energy loss as a function of fiber content.  $\sigma_0 = 0.2$  MPa, vibration frequency 10 Hz. Symbols as in Figure 1.



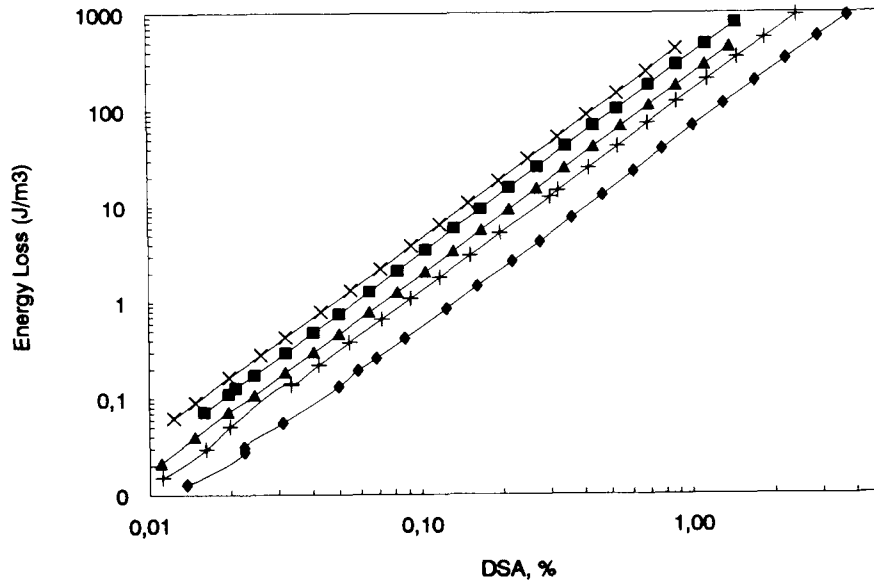


Figure 8 Energy loss variation as a function of strain amplitude. (♦) C-1; (+) C-6; (▲) C-7; (■) C-8; (X) C-9, longitudinal measurements.

CONCLUSIONS

Polyester PET fiber treatment with 1,4-carboxy-sulphonyl diazide gives rise to treated fiber-matrix bonds during the curing process. These bonds become manifest in the variation of the dynamic properties of the material measured at variable dynamic strain amplitude.

In fact, when comparing the dynamic properties of composite materials containing untreated and treated fiber at variable strain, although the behavioral pattern follows the same trend in both cases, the differences are to be found in storage modulus  $E'$  variation, which shows higher values for treated fiber composites, in longitudinal as well as in transversal measurements, and a less prominent drop as

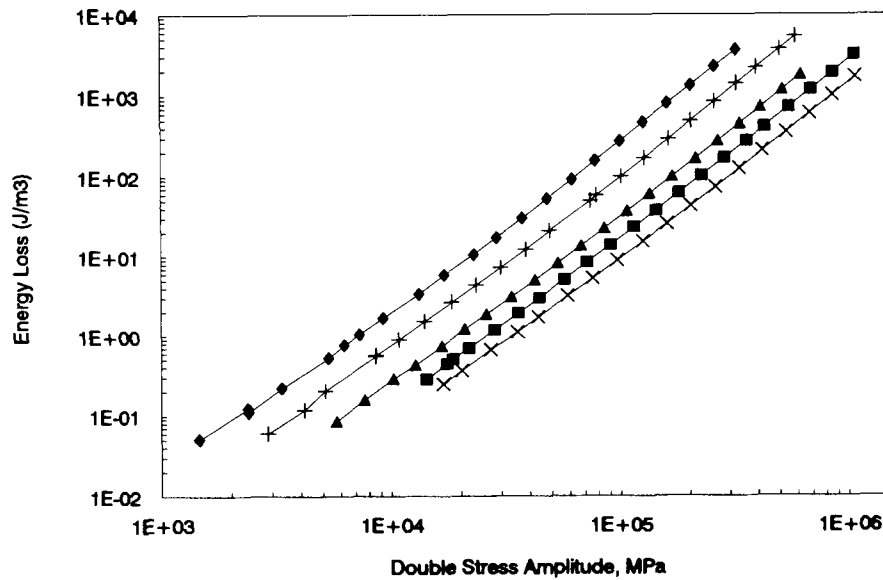


Figure 9 Energy loss variation as a function of stress amplitude. Longitudinal measurements. Symbols as in Figure 8.

a result of increased strain amplitude, as well as a lesser increase in the loss factor,  $\tan \delta$ , which translates into greater strength of the interface capable of resisting substantial strain.

The  $E'_T$  modulus of the composites may be expressed by means of the logarithmic blend rule and hence the value of a factor indicating the degree of matrix-fiber bonding can be determined, a factor which proves to be greater for the composites filled with treated fiber.

These composites can also be applied to the method developed by Zhov et al.<sup>23</sup> for equivalent interfacial thickness determination,  $\Delta R$ , which is higher for the materials containing treated fiber, i.e., the modification achieved in the fibers enhances interfacial activity. Equivalent interfacial thickness diminishes with increasing dynamic strain amplitude. Yet the reduction is milder for treated fiber composites, implying better retention or else smaller drops in their properties.

By the same token, phase bonding gives rise to energy dissipation, i.e., to a loss in mechanical energy, at constant strain amplitude, to a lesser degree at constant stress amplitude, which obliges to differentiate between the type of deformation involved, i.e., stress or strain, when speaking of energy dissipation.

For any type of composite, energy loss increases with increasing fiber content.

The author gratefully acknowledges partial financial support of this research by CICYT and the Regional Government of Madrid.

## REFERENCES

1. D. K. Setua and S. K. De, *Rubber Chem. Technol.*, **56**(4), 808 (1983).
2. T. S. Solomon, *Rubber Chem. Technol.*, **58**(3), 561 (1985).
3. M. Tsukuda, T. Yamamoto, N. Nakabayashi, H. Ishikawa, and G. Freddi, *J. Appl. Polym. Sci.*, **43**, 2115 (1991).
4. C. D. Papaspyrides and J. Poutakis, *Polym. Int.*, **27**, 139 (1992).
5. A. Beshay and S. V. Hoa, *Sci. Eng. Composite Mat.*, **2**(2), 85 (1992).
6. J. D. Miller, H. Ishida, and F. H. J. Maurer, *Polym. Composites*, **9**(1), 12 (1988).
7. V. M. Murty and S. K. De, *Rubber Chem. Technol.*, **55**(2), 287 (1982).
8. S. Akhtar, P. P. De, and S. K. De, *J. Appl. Polym. Sci.*, **32**, 5123 (1986).
9. A. Y. Coran, K. Boustany, and P. Hamed, *J. Appl. Polym. Sci.*, **15**, 2471 (1971).
10. B. Das, *J. Appl. Polym. Sci.*, **17**, 1019 (1973).
11. V. M. Murty, S. K. De, S. S. Bhagawan, R. Sivaramakrishna, and S. K. Athithan, *J. Appl. Polym. Sci.*, **28**, 3485 (1983).
12. M. Ashida, T. Noguchi, and S. Mashimo, *J. Appl. Polym. Sci.*, **30**, 1011 (1985).
13. F. Rybnikar, *Angew. Makromol. Chem.*, **191**, 31 (1991).
14. A. Hampe and C. Marotzke, *Polym. Inter.*, **28**, 313 (1992).
15. M. Arroyo, M. Tejera, and L. Ibarra, *J. Appl. Polym. Sci.*, **48**, 1019 (1993).
16. L. Ibarra, *J. Appl. Polym. Sci.*, **49**, 1595 (1993).
17. L. Ibarra and C. Jordá, *J. Appl. Polym. Sci.*, **48**, 375 (1993).
18. E. Palma and L. Ibarra, *Angew. Makromol. Chem.*, **220**, 111 (1994).
19. A. I. Medalia, *Rubber Chem. Technol.*, **51**(3), 437 (1978).
20. L. Ibarra and C. Chamorro, *J. Appl. Polym. Sci.*, **43**, 1805 (1991).
21. J. Kubat, M. Rigdahl, and M. Welander, *J. Appl. Polym. Sci.*, **39**, 1527 (1990).
22. M. Ashida, T. Noguchi, and S. Mashimo, *J. Appl. Polym. Sci.*, **29**, 661 (1984).
23. Y. H. Zhou, T. Chen, W. D. Wu, C. Li, D. H. Li, and Q. Zhang, *Macromol. Rep.*, **A30**(suppl. 5), 365 (1993).
24. S. Futamura, *Rubber Chem. Technol.*, **64**(1), 57 (1991).
25. L. Ibarra, *Kauts. und Gummi Kunstst.*, **45**(12), 1061 (1992).

Received April 18, 1994

Accepted July 7, 1994